sciendo

Geologos 31, 2 (2025): 119–135
https://doi.org/10.14746/logos.2025.31.2.10

GEOLOGOS

Geological controls and exploration strategies for sandstone-type uranium ores: comparison of Indian deposits with those across the globe

Shreya Sharma, Rishikesh Bharti*

Department of Civil Engineering, Indian Institute of Technology Guwahati, Guwahati 781039, India
*corresponding author, e-mail: rbharti@iitg.ac.in

Abstract

The rising global energy demand has driven researchers to locate new uranium deposits, with sandstone types contributing nearly 40 per cent of uranium production. The present review provides a comprehensive understanding of the genesis and classification and mentions some global examples of sandstone-type uranium deposits, the focus being on the geological settings of each type. Understanding these factors helps locate similar deposits, especially in North-East India, where research is limited. There, uranium enrichment is controlled by numerous factors such as source rocks, sedimentary structures, permeability barriers, reductants and cap rocks. The present study underscores the need for integrated methods for exploration of sandstone-type deposits where remote sensing can be combined with geophysical and geochemical techniques.

Keywords: Uranium ore genesis; structural controls, integrated exploration techniques; North-East India

1. Introduction

As global energy demands surge, the transition to cleaner energy sources is becoming increasingly important. Nuclear power is poised to play an important role in this transition, driving the need for uranium exploration and extraction. Among the various uranium deposit types, sandstone-hosted ones are of significant economic importance (Dai et al., 2015), accounting for approximately 18 per cent of the world's uranium resources and 43 per cent of the grand total of known deposits (Raju, 2019). These deposits, primarily composed of uraninite and coffinite, occur in fluvial, alluvial, marginal marine and lacustrine environments, predominantly in the USA, Australia, Kazakhstan, China and Africa (Finch & Davis, 1985; Hou et al., 2017). Palaeozoic strata are less common and are found mostly as roll-front deposits in Western Australia and Europe (IAEA, 2009; Hou et al., 2017). Thus, the known distribution of U deposits and occurrences relies on data by the International Atomic Energy Agency (Fig. 1; IAEA, 2021).

A widely accepted model for sandstone-type deposits was developed long ago; it has helped discover such deposits worldwide (IAEA, 2009; Penney, 2012). Key points in the deposition of uranium include: (i) A fluvial-lacustrine depositional environment in intermontane basins, marginal marine plains and intracratonic piedmonts; (ii) uranium-rich basement rocks as primary sources; (iii) uplift period resulting in erosion, fluvial channel development and groundwater downward flow; (iv) the presence of reducing agents such as organic matter and authigenic pyrite; and (v) porous sandy host rocks, facilitating uranium precipitation at redox fronts.

Uranium mineralisation occurs through redox reactions, where U(VI) is reduced to U(IV), lead-

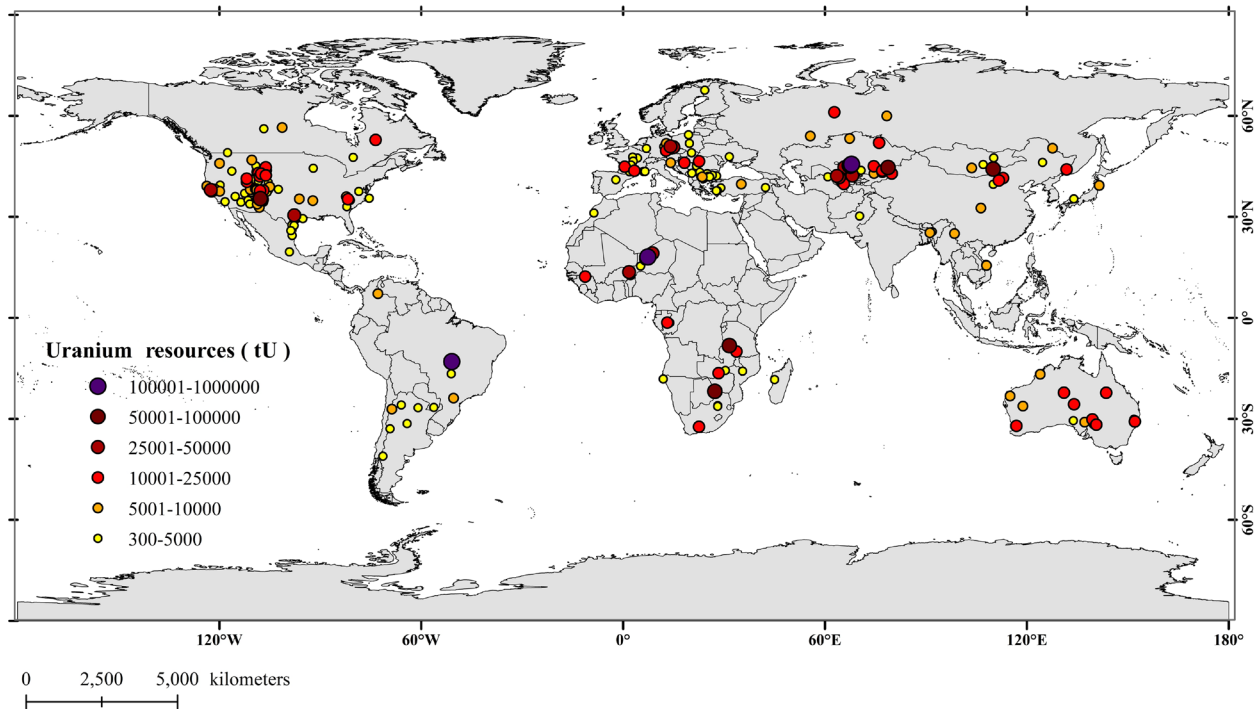

Fig. 1. Global U-abundance map of sandstone-type deposits. Data source: World Distribution of Uranium Provinces, IAEA (2021).

ing to precipitation. Organic matter, biogenic and non-biogenic H_2S, and hydrocarbons play critical roles as reductants (Spirakis, 1996; Cuney, 2010). Hydrocarbon-rich basins have been linked to uranium deposition, with petroleum-related gases contributing to mineralisation processes (Jaireth et al., 2008; Bonnetti et al., 2015). Hydrothermal uranium deposits, including basal-type, tabular, roll-front and tecto-lithologic types, further demonstrate the diverse pathways of uranium enrichment.

2. Sandstone-type uranium deposits: examples from across the globe

Sandstone-type uranium deposits rank among the most significant across the globe. These deposits typically form in fluvial, lacustrine or marginal-marine settings, with uranium sourced from nearby felsic or U-rich rocks. In such deposits, groundwater plays a crucial role in the transportation and precipitation of U-rich fluids in the host rock in a reduced state. The geological characteristics of sandstone-type uranium deposits are highlighted in Table 1.

2.1. Generalised characteristics of sandstone-type uranium deposits

The host rocks of sandstone-type uranium deposits usually are medium- to coarse-grained sandstones that are highly porous and permeable, crucial for the movement of groundwater. The various tectonic settings in which such rocks are found include continental platforms and intermontane or sag basins in a stable environment (IAEA, 2020). The sandstones can be poorly consolidated or entirely unconsolidated in the case of roll front deposits, or they can show traces of overgrowths and pressure solutions for tabular deposits when they are lithified, indicative of deep burial.

Different felsic rocks are found to be associated with uranium mineralisation. Crystalline basement rocks, such as granitoids, are primary sources of uranium. U-rich granites are observed in the periphery of sandstones in intermontane or intercratonic basins. These are responsible for initial U enrichment. Pegmatites and leucogranites are other important felsic rocks that are uranium-rich, having formed from partially melting Palaeoproterozoic metasediments. The uranium found in these deposits is usually seen in association with elements such as vanadium, molybdenum, copper and others. The fluids involved in uranium genesis range from

Table 1. Generalised characteristics of sandstone-type uranium deposits.

Characteristics	Description	References
Depositional environment	Fluvial, lacustrine, shallow-marine sedimentary settings	Dahlkamp (2009), IAEA (2020)
Geological settings	Varying basin settings such as intracratonic basins, intermontane basins or continental margin basins	Dahlkamp (2009), IAEA (2020), Jaireth et al. (2008)
Age	Paleozoic to Cenozoic (except for mafic dykes/ sills in Proterozoic sandstones: Paleo- to Mesoproterozoic)	IAEA (2020)
U mineralization	Usually follows bedding planes but can cut across to form roll-fronts	Finch & Davis (1985)
Sources of U	Uranium-rich felsic rocks rimming/underlying the basin Lithic fragments of the felsic rocks (including the volcanic ash) in the sandstone aquifer Leachable detrital U-rich minerals (apatite, zircon, allanite) Felsic volcanics near the sandstone aquifer Uranium occurrences in the hinterland	Skirrow et al. (2009)
Factors for U mobilization	Fluid-rock ratio Geochemistry of granite (peraluminous/ peralkaline) Oxidizing conditions (Eh factor)	Porwal & Carranza (2015)
Transport medium	Groundwater/meteoric water (oxidizing, variable salinity, neutral to moderately acidic pH)	Jaireth et al. (2008)
Reductants	Solid carbonaceous material such as coal, woody material, humic/ humate components Hydrocarbons and/or H_2S from the reservoirs or coal seams and focussed into the site of deposition along the different pathways like local structures and the permeable facies Inorganic reductants such as Fe^{2+} rich rocks, sulphides especially pyrite and/or H_2S	Skirrow et al. (2009)
Host rock	Quartzose to feldspathic to arkosic sandstones, may contain acidic volcanic material, medium- coarse-grained	Finch & Davis (1985), IAEA (2020)
Associated metals	Vanadium, silver, copper, molybdenum, selenium	Evans (2009)
Dominant U minerals	Uraninite, coffinite, uraniferous hydrocarbons and associated with vanadium minerals	Boyle (1982)

shallow oxidised alkaline to reduced groundwaters and hydrocarbon-bearing brines (IAEA, 2020). Uranium distribution is thus controlled by the oxidation states of the sandstone and the flow of oxidising fluids, which is further controlled by sandstone porosity and permeability. Other factors that exert significant impact include structural and lithological controls (IAEA, 2020).

Sandstone-type deposits can be subdivided into different sub-types based on morphology, such as roll front or tabular type, or on sedimentological settings, e.g., palaeochannel, palaeovalley or unconformity or lithological or tectonic controls, for instance tectonolithological or mafic dykes and sills (IAEA, 2020; Cuney et al., 2022).

2.2. Basal channel type

Palaeovalley systems, which are filled with highly permeable and poorly consolidated fluvial sediments, show the presence of basal channel deposits. Ore deposits are seen in association with plant remains that act as a reductant and form stratiform deposits (IAEA, 2020). Deposits in South Australia, such as Beverley and Four Miles, are examples of basal channel type deposits. They show distinct features, here summarised in Table 2.

The Beverley Deposit, situated in the Lake Frome Basin's terrestrial sediments in the North Flinders Range of South Australia, shows this type of mineralisation and is located about 13 km away from the uranium-enriched Mount Painter Inlier's Mesoproterozoic basement. Deposition of uranium mineralisations is confined to the organic-poor lacustrine sands of Miocene age, as well as to a portion of the underlying reductive strata composed of silt and organic-matter-rich clays (Wülser et al., 2011). Possible uranium sources include a) the Mount Painter domain basement, b) Miocene formations and c) Willawortina Formation alluvial fans, although the Mount Painter Inlier basement is the most widely accepted source (Wülser et al., 2011). The major uranium mineral is coffinite which occurs both as void fills, as well as quartz grain coatings (Penney, 2012). Uranium mineralisation is found in tabular as well

Table 2. Various basal channel deposits and their characteristics.

Characteristics of deposits	Description	References
Beverley Deposit (Lake Frome Basin, Callabonna Sub-basin, South Australia)	Located ~13 km from uranium-enriched Mount Painter Inlier's Mesoproterozoic basement. Host rock: Mineralization is in organic-poor lacustrine sands (Late Oligocene to Miocene age). Reductive strata contain silt and organic-rich clays. Tabular and channel deposit sub-type.	Wülser et al. (2011), Penney (2012)
Uranium sources	Mount Painter domain basement (widely accepted) – granites and granitoids. Miocene formations – silts and sands (angular and immature), smectite rich, partly magnesian clay and dolomite. Willawortina Formation alluvial fans – varying from fine sands and clay to coarse siliciclastics, heavy minerals present too.	Hochman & Ypma (1987), Wülser et al. (2011)
Primary uranium mineral	Coffinite (found as void fills and quartz grain coatings)	Penney (2012)
Ore zone characteristics	Tabular and lenticular mineralization, mainly in contact with organic-rich Alpha Mudstone. The uncemented grey sand contains marcasite, pyrite, clays, feldspar, alunite, and gypsum. Later oxidation led to carnotite formation.	Penney (2012)
Four Mile Deposit (West of Beverley, South Australia)	Australia's largest sandstone-hosted uranium resource. Dominant ore mineral: uraninite, associated with kaolinite, pyrite, REE, and U-bearing phosphate minerals.	Penney (2012), Hou et al. (2017)
Host rock of Four Mile West	Upper Cretaceous sands of Bulldog Shale (Eromanga Basin's topmost unit)	Hou et al. (2017)
Host rock of Four Mile East	Palaeochannel sands of Eyre Formation (Pliocene-Eocene), composed mainly of mature sands with abundant pyrite and carbonaceous matter.	Penney (2012)

as lenticular zones, especially in contact with the organic-rich Alpha Mudstone. The ore zone's uncemented grey sand comprises marcasite, pyrite, feldspar, alunite and gypsum, where the two last-named may have been related to a later oxidation stage which resulted in the production of carnotite (Skirrow, 2009).

The Four Mile, located to the west of Beverley, is considered the largest and highest sandstone-hosted uranium resource in Australia. This deposit has two distinct zones, namely the Four Mile West and Four Mile East. The dominant ore mineral found is uraninite, in association with pyrite and kaolinite, along with a variety of rare earth elements and U-bearing phosphate minerals (Penney, 2012; Hou et al., 2017). The host rock of the Four Mile West Deposit is Upper Cretaceous sands of the Bulldog Shale which is the highest unit of the Eromanga Basin (Jaireth, 2009). In contrast, Four Mile East lies in palaeochannel sands of the Eyre Formation, of Eocene to Pliocene age (Penney, 2012). The Eyre Formation present in this deposit consists mostly of mature sands with abundant pyrite and carbonaceous matter, in comparison to the Beverley sands.

2.3. Tabular type

Peneconcordant or tabular deposits form in braided fluvial systems and are mostly seen to overlie sedimentary or crystalline rocks unconformably. The mineralised zone occurs as lenticular or tabular masses and is mainly parallel to deposition trend (Dahlkamp, 2009). The deposits present in the Tim Mersoi Basin of Niger are typical examples of tabular type U mineralisations (Mamadou et al., 2022). The various characteristics of such deposits are here outlined in Supplementary Table (see Geologos website), along with genetic models.

The genetic models of the Akouta uranium deposit propose different ages and depositional mechanisms for mineralisation (Mamadou et al., 2022). The first model, based on a Pb-Pb age of 338±5 Ma, suggests a synsedimentary origin with uranium sourced from the basin and deposited contemporaneously with Carboniferous sedimentation (Fig. 2A; Devillers & Menes, 1977). Cazoulat (1985) proposed an initial uranium preconcentration stage, with U leached primarily from Ordovician volcanic rocks in the Air Mountains and deposited within or-

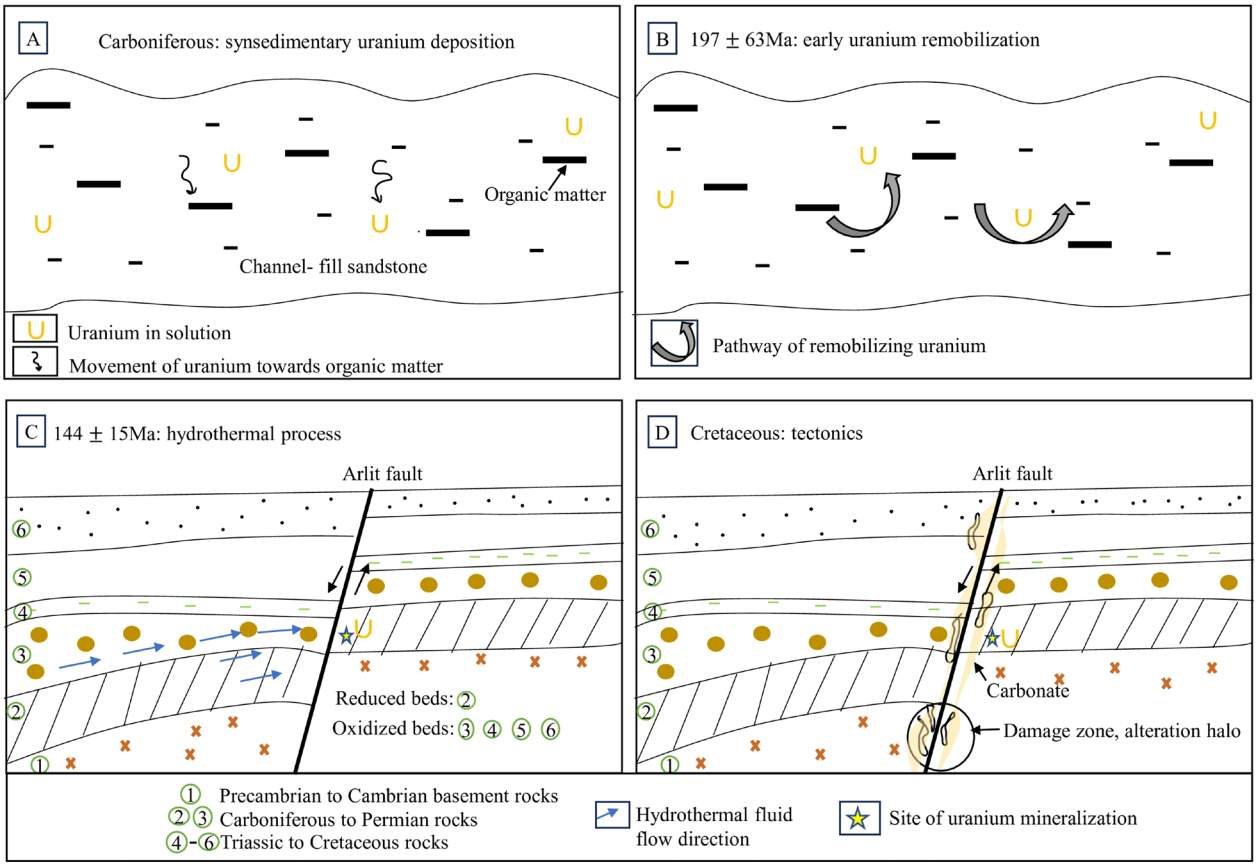

Fig. 2. Genetic models of the Akouta uranium deposit. **A –** Synsedimentary uranium deposition (Devillers & Menes, 1977); **B –** Early uranium remobilisation (Turpina et al., 1991); **C –** Diagenetic/hydrothermal process (Forbes, 1989); **D –** The role of tectonics (Gerbeaud, 2006). Layer 1 depicts argillite formation and layers 2–5 refer to the formations with dominant coarse-grained sandstones, with layer 5 having abundant clay (modified after Mamadou et al., 2022).

ganic-rich fluvial and deltaic sandstones. A second model, supported by a U-Pb age of 197±63 Ma, suggests early remobilisation of a pre-existing uranium source (Fig. 2B; Turpina et al., 1991). Forbes (1989) proposed a third model which involves uranium remobilisation through diagenetic or hydrothermal processes, facilitated by movements along the Arlit fault (Fig. 2C). This model, supported by a U-Pb age of 144±15 Ma, suggests that faulting induced the interaction between oxidised Permo-Jurassic formations in the west and reduced Carboniferous formations in the east, promoting uranium deposition. Finally, Gerbeaud (2006) emphasised the role of Cretaceous-aged tectonics in fluid mobilisation, inferred from structural features such as extensive fracturing, cemented fractures and a carbonate halo adjacent to the Arlit fault. However, this model lacks absolute age constraints (Fig. 2D).

Another important tabular deposit is found in Colorado, United States. The Colorado Plateau hosts more than 4,000 uranium occurrences (Hall et al., 2023) in the region and ranks among the largest uranium provinces in the world. The uranium deposits are hosted by quartzose to arkosic sandstones of the Chinle Formation of Triassic age and Morrison Formation of Jurassic age. The uranium deposits are usually associated with vanadium and are generally distinguished by high vanadium-to-uranium ratios. The Colorado Plateau also shows the presence of basal channel deposits and very minor roll-type deposits. The ore mineralogy includes uraninite, coffinite, montroseite and chalcocite (Finch, 1996).

2.4. Roll front type

These sandstone deposits refer to uranium accumulation in medium- to coarse-grained sedimentary rocks that cross-cut sandstone bedding and extend vertically between overlying and underlying horizons. When observed in cross-section, these deposits are crescent-shaped. The ores occur as disseminations on the redox front's downgradient side. Such roll-front uranium deposits are seen in some basins in Kazakhstan and China and are

Table 3. Various examples of roll-type uranium deposits.

Deposit location	Geological features	Host rock	Origin	U minerals & associated minerals	References
Chu-Sarysu Basin, Kazakhstan	Sequence of clay, gravel and sandstone (Cretaceous-Paleogene). ~5 km thick Palaeozoic basement	Sandstone	Regional oxidation zone. Reduced fluids (hydrocarbons, H_2S) create geochemical traps.	Coffinite, pitchblende, sooty pitchblende, pyrite, marcasite, calcite	Jaireth et al. (2008), Dahlkamp (2009)
Syrdarya Basin, Kazakhstan	Bounded by Karatau Range (NE) and Tien Shan (S). Coastal-marine & continental sediments up to 3000 m thick.	Arenites	Controlled by dynamic roll fronts. Multi-stage oxidation tongues in aquifers.	Uraninite, pyrite, marcasite, calcite, V, As, Se in oxidized sands, Mo in reduced portions	Petrov (1998), Dahlkamp (2009)
Erlian Basin, NE China	Intracontinental basin. Alternating sandstone and mudstone layers.	Sandstone	Uranium sourced from nearby granitic and felsic rocks. Weathering and leaching play a role.	Coffinite, pyrite, organic matter	Wu et al. (2005), Hou et al. (2017), Nie et al. (2020)
Ordos Basin, N China	Mesozoic intracratonic basin developed on Palaeozoic sedimentary rocks. Precambrian basement.	Feldspathic sandstone	Redox regime influenced by tectonic activity. Uplift promoted oxidation front movement.	Coffinite, pitchblende Fe^{2+}, CH_4, H_2S, micro-bacteria-related U precipitation	Akhtar et al. (2017), Hou et al. (2017)
Yili Basin, NW China (Xinjiang)	Mesozoic basin. Channel facies of braided delta system.	White & brown sandstones	Transitional redox zone with enriched Mo & Se. Coal-bearing Jurassic sediments host uranium deposits.	Pitchblende, coffinite, U-bearing sulphate, dolomite, calcite, limonite, ilmenite	Dahlkamp (2009), Dai et al. (2015), Shi et al. (2020)
Powder River, Wyoming USA	Intermontane basin. Synclinal basin underlain by fluvial Eocene Wasatch Formation (sandstone lenses present). U deposits within the lenses and associated with hematite red zones.	Medium to coarse grained arkosic sandstones	Release of U from the devitrification of volcanic ash in the overlying formations or from the granitic terranes by groundwater. Concentration of U through intralens accretion and formation of roll fronts (oxygenated water in reducing condition).	Uraninite, coffinite, carnotite, uranophane, pyrite	Sharp et al. (1964), Santos (1981)
Wind River Basin, Central Wyoming USA	A trapezoidal-shaped structural depression surrounded by several Laramide structures that include Wind River. The presence of northwest trending anticlines.	Arkosic sandstone	Deposits formed within the porous and permeable sediments. Oxygenated groundwater dissolved U from the granites and tuffs. Mineralization at the redox front upon encountering the reductant pyrite.	Uraninite, coffinite, autunite, pyrite	Seeland (1978, 1986), Gregory (2024)
Shirley Basin, Wyoming USA	Syncline (the Laramide orogeny, Cretaceous to Paleogene) with huge U deposit. Significant unconformity - the palaeotopographic erosional surface with channel and overbank deposits.	Arkosic sandstone	Roll front from oxygenated meteoric water that dissolves U from overlying volcanic tuffs and adjoining granitic rocks. It precipitates at the redox boundary when it encounters organic matter and pyrite.	Uraninite, coffinite, carnotite pyrite	Harshman (1966, 1972), Covington & Kennelly (2018)

primarily associated with formations generally referred to as red beds and formed by oscillation of the red-ox front. The reddish colour is imparted by iron-rich minerals in the sedimentary formations. The red beds represent an oxidising environment such as fluvial channels or arid continental settings. The oscillation of the redox front is responsible for the formation of uranium deposits within the red beds. The soluble U^{6+} is transported in groundwater until it encounters the reductants such as organic matter or pyrite where it precipitates as U^{4+} minerals such as coffinite or uraninite. The cycle of migration and precipitation is controlled by the position of the redox interface as well as by movement over geological time. These become the genesis of roll-front-type uranium deposits that occur in red bed settings (Cuney & Kyser, 2009; Dahlkamp, 2009). Table 3 summarizes the characteristics found in these basins.

The Ordos Basin in north-central China formed as a result of the collision of the Tethys orogen with the North China and Yangtz blocks (Akhtar et al., 2017). This Mesozoic intracratonic basin, underlain by a Precambrian basement, hosts oil, gas, coal and uranium (Hou et al., 2017). Uranium deposits, primarily in the Zhilou Formation, formed due to Jurassic–Early Cretaceous tectonic activity, creating redox mineralisation conditions. Faults acted as hydrodynamic discharge zones and geochemical barriers essential for interlayer oxidation (Akhtar et al., 2017). The dominant uranium mineral, coffinite, occurs at grey-green and grey sandstone transitions (Hou et al., 2017). Uranium precipitated as oxidised fluids encountering reductants such as H_2S, CH_4, Fe^{2+}, organic carbon and microbial activity (Fig. 3; Akhtar et al., 2017).

Shi et al. (2016) proposed a supergene hydrothermal model linking coal combustion-induced burnt rocks to the alteration of underlying sandstones in the interlaminated oxidised zone (Shi et al., 2020). Past dry climatic conditions led to coal self-ignition, while subsequent humid conditions allowed groundwater to infiltrate heated permeable rocks, forming an oxidised zone marked by reddish sandstone (Fig. 4; Shi et al., 2020). This process dissolved uranium and other ions from altered coals and burnt rocks, which were then transported by heated fluids. Uranium precipitation occurred in the lower sandstone layers due to fluid cooling and redox reactions, forming transitional white sandstone through diagenetic changes (Shi et al., 2016). The cooling of supergene hydrothermal fluids enriched in U, Mo and Se resulted in vertically zoned ore bodies resembling hydrothermal uranium deposits (Dai et al., 2015; Shi et al., 2020).

Kazakhstan produces more than 40 per cent of the world's uranium and has about 14 per cent of global uranium resources. The Chu-Sarysu and Syrdarya basins host significant roll front-type of deposits in the south-central portion of the country. These basins were once part of an extensive artesian system but were split due to Pliocene uplift of the Karatau Mountains (Dahlkamp, 2009). Uranium deposits occur in thick, permeable Upper Cretaceous and Paleocene-Eocene sandstones capped by the impermeable shales. These deposits are poor in organ-

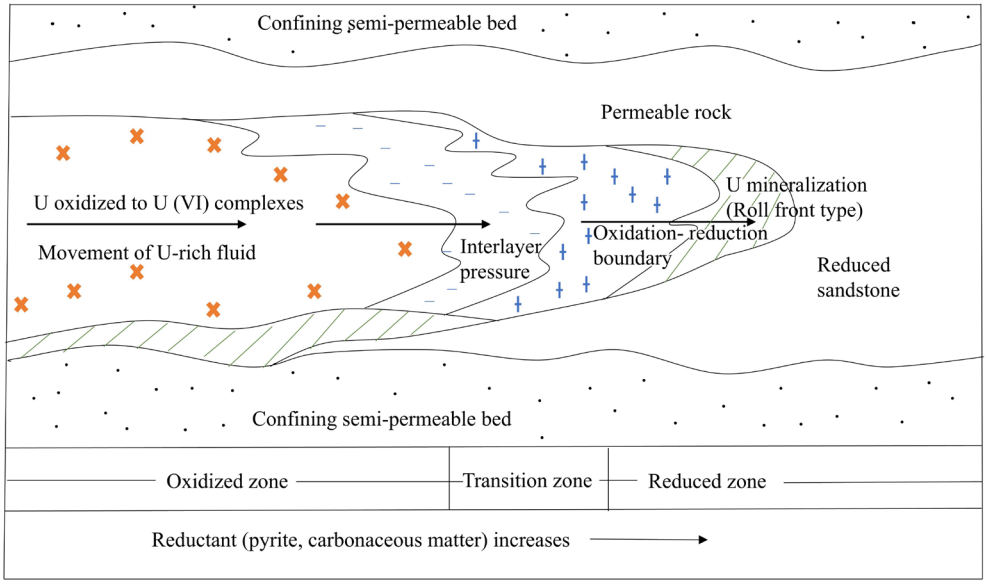

Fig. 3. A model showing permeable rocks of the Zhilou Formation with roll front-type uranium mineralisation under reducing state (modified after Akhtar et al., 2017).

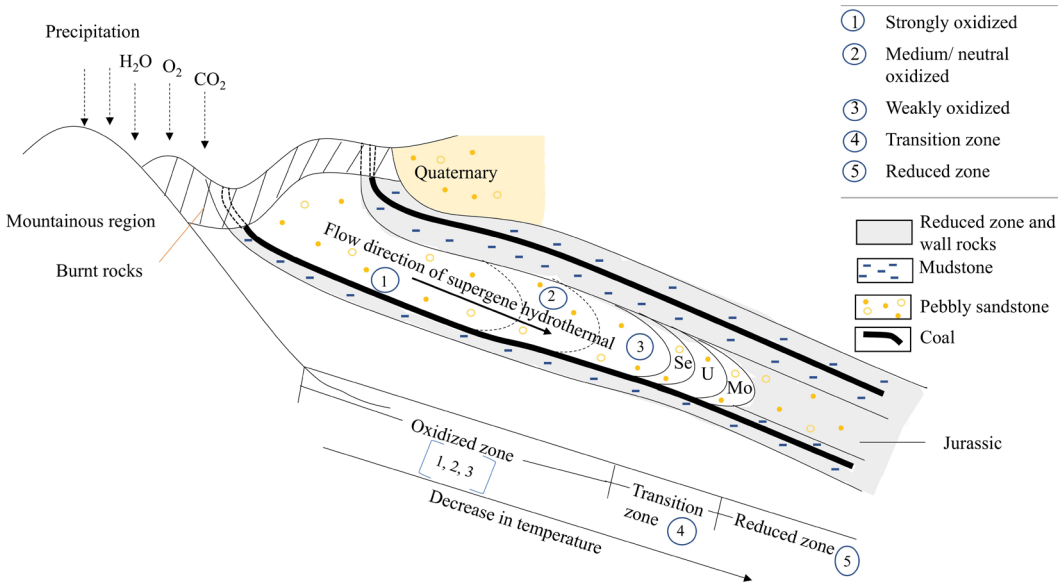

Fig. 4. Uranium mineralisation in the Yili Basin. The process shows supergene hydrothermal fluid model following coal combustion (modified after Shi et al., 2020).

ic matter. Here, hydrocarbons, along with H_2S, are the vital reductants that form the geochemical trap. The redox fronts highly control the mineralisation in such terrains. The oxidation zone comprises iron hydroxides, while the main reductants are pyrite and marcasite. Enrichment of zinc, copper, cobalt, rhenium, silver, nickel, molybdenum and vanadium is observed, in addition to notably enriched selenium occurring near the contact of reduction zones (Jaireth et al., 2008). The uranium mineralisation is in the form of fine coffinite and pitchblende, disseminated in clay matrix and sandstone infill cavities (Petrov, 1998). Most of the sandstone-type uranium deposits are extracted using *in-situ* leaching.

Another classic example of the redox front includes Wyoming, United States, the second-largest uranium province after the Colorado Plateau (Dahlkamp, 1993). Major regions with high uranium deposits include the Powder River, Wind River, Shirley, Great Divide and Washakie basins. In the Great Divide Basin, uranium resources are primarily found in sandstones of the Eocene Battle Spring Formation. The genesis of these deposits is believed to be linked to the Granite and Laramie Mountains. Oxidising groundwater solutions carried dissolved uranium through the host rocks, i.e., weakly lithified sandstones. Deposition of these formations occurred as alluvial fans with abundant carbonaceous debris and pyrite that helped reduce the environment for precipitation. Uranium mineralisation is observed at the redox fronts with pitchblende and coffinite being the primary uranium minerals, which coat sand grains and occupy void spaces (Abzalov & Paulson, 2012). These deposits formed in the Great Divide Basin during the Oligocene.

2.5. Tectonolithologic deposits

Such ore bodies are controlled by both host lithology and tectonic structures (Cuney et al., 2022). These sandstone deposits are discordant in nature and are found mainly along permeable zones with tongue-like impregnations extending to the host rock away from faults. The redistribution of primary uranium into the permeable zone results in a thick and steeply dipping deposit known as a stack deposit. Strong structural and lithological permeability controls are observed in these deposits in the mineralisation process. The hydrocarbon traps significantly control the localisation and generation of U deposits (IAEA, 2020).

The Franceville Basin in southern Gabon hosts uranium mineralisations and is bounded by crystalline terrains to the north and south, with the Bateke Plateau to the east and the metamorphic Ogouué System to the west. The basin contains the Franceville Series, an unmetamorphosed volcanoclastic sedimentary sequence of Early Palaeoproterozoic age, with a thickness of 1–2.5 km (Bankole et al., 2016). The Franceville sub-basin can be further divided into five formations, ranging from FA to FE, in ascending order. Among these, the FA Formation consists of two main units, i.e., a sandstone-dominated succession of fluvial origin and overlying sandstones and shales of fluvio-deltaic-tidal suc-

cession. The overlying FB Formation consists of black shales. Uranium mineralisation in the basin is primarily associated with organic matter, and evidence of past petroleum activity is indicated by tectonic and lithostratigraphic characteristics of the basin, along with the presence of carbonaceous ore. Studies suggest a genetic link between uranium, organic matter, thermal maturity and oil migration, with multiple oil generation and migration phases followed by fluid mixing and hydrofracturing facilitating uranium mineralisation (Lecomte et al., 2020). Major uranium deposits in the Franceville Basin including the Oklo deposit, are closely associated with organic matter. Gauthier-Lafaye & Weber (1989) proposed that oxidised uranium-bearing fluids percolated through FA Formation fractures, where interaction with organic matter reduced U^{6+} to U^{4+}, leading to precipitation of uraninite and pitchblende. The FA Formation unconformably overlies Archean granitoid basement rocks and consists of fine- to coarse-grained sandstones, conglomeratic sandstones and thinly interbedded mudstones (Bankole et al., 2016). Uranium ore formation in the lower Proterozoic Franceville Basin is closely linked to petroleum migration within a hydrocarbon system, with mineralisation controlled by multistage mixing between uranium-bearing brines and hydrocarbons, influenced by sandstone porosity and hydrofracturing (Lecomte et al., 2020). Gauthier-Lafaye (2006) discussed various redox-controlled uranium mineralisation models, considering factors such as increased atmospheric oxygen during the Great Oxidation Event, uranium leaching from conglomeratic sandstones in a fluvial setting, uranium mobilisation by oxidised fluids through fractures and permeable zones, and subsequent precipitation in the FA Formation upon interaction with hydrocarbons sourced from the FB formation (Bankole et al., 2016).

2.6. Mafic dykes/sills

Uranium mineralisation generally is related to mafic dykes and sills and occurs as discordant or concordant structures in relation to the Proterozoic sandstone. Thus, mineralisation is in the form of veins, disseminated or semi-massive nature, and is hosted by coarse-grained fluvial sandstones as well as conglomerates apart from mafic dykes and sills along with contact zones of these lithologies.

The Matoush uranium deposit, located in the Otish Basin (Quebec, Canada), represents a sandstone-hosted uranium deposit characterised by a sheet-like ore body that is spatially associated with the Matoush fractures and altered portions of the Matoush dykes (Alexandre et al., 2015). The Indicator Formation sandstone and the mafic dykes exhibit alteration mineralogy, including Cr-rich muscovite and dravite, with uraninite as the primary uranium mineral, closely associated with eskolaite. The mafic dyke plays a dual role as a reductant for uranium precipitation and as a source of Fe and Cr. The deposit is confined to the Indicator Formation of the Otish Group, which overlies unconformably the granitic basement. Potential uranium sources include refractory minerals such as zircon, monazite and apatite within the Indicator Formation, the Superior Province basement rocks and the Matoush dyke. However, the pegmatitic portion of the dyke is considered an unlikely source due to its low uranium content and volume (Alexandre et al., 2015). The mobilisation and transport of uranium occurred via oxidising basinal fluids circulating through the Indicator Formation, as indicated by low Th/U ratios and δ^2H values. Uranium mineralisation is restricted to specific horizons above the unconformity, with minimal alteration observed in the basement rocks, suggesting limited fluid penetration. Uranium was likely leached from refractory phases by oxidising brines and transported to the depositional site within highly permeable, coarse-grained lithofacies intersecting the Matoush Fracture, acting as a conduit for uranium-bearing fluids. Mineralisation occurs in two forms: (i) massive to semi-massive lenses and pods associated with the mafic dyke and (ii) disseminated mineralisation within the hydrothermal alteration halo, where Cr-rich muscovite and dravite contributed Fe^{2+}, facilitating the reduction of U^{6+} to uraninite.

3. Identification of primary and secondary sandstone-type uranium in North-East India

The sandstone-type uranium deposits are found primarily in the Mahadek Basin in Meghalaya, North-East India. This basin is an uplifted, horst-like feature that bounds the Brahmaputra Valley to the north and the Surma Valley to the south. The Upper Cretaceous Mahadek Formation hosts uranium mineralisations, and the host rocks are coarse-grained feldspathic arenites containing organic matter and altered pyrite, overlying Precambrian granites and gneisses. The primary uranium sources are the South Khasi Batholith and Neoproterozoic granitoids, which provide leachable uranium. Mineralisation occurs as coffinite and pitchblende,

associated with low-rank organic matter, biogenic framboidal pyrite, melnicovite pyrite, galena and chalcopyrite, with some uranium also being present in organic matter and secondary uranium minerals. The region shows uranium mineralisation such as uraninite, coffinite, brannerite, autunite, meta-autunite, torbernite, meta-torbernite and others (Raju, 2019). The Mahadek Formation is divided into Upper and Lower Mahadek sediments, representing oxidising marine and reducing fluvial environments. The Upper Mahadek sediments comprise purple sandstones intercalated with shale and clay, cemented by glauconite. The Lower Mahadek sediments consist of arenaceous strata with fluvial structures, including cross-bedding and scour-and-fill features. It hosts the most significant uranium mineralisation, particularly within braided channels and deltaic environments. Key factors controlling uranium mineralisation include the following:

- *Fertile provenance*. Uranium is sourced from Meso- to Neoproterozoic granitic rocks with radioelement concentrations of 2.9–11.3 ppm. Additional sources include carbonaceous slates and metasedimentary rocks (sericite schist) (Raju, 2019).
- *Fluid transport distance*. U-mineralisation depends on the transport distance of uranium-bearing fluids. Proximal deposits are less mature and poorly sorted, while distal deposits are well sorted with minimal cement.
- *Plateau* vs. *escarpment region*. Plateau settings favour larger tonnage and higher-grade deposits compared to Escarpment regions.
- *Reductants*. Organic matter, pyrites (framboidal, melnicovite) and sulphides provide reducing conditions necessary for uranium precipitation.
- *Structural controls*. Faults, lineaments and other basement features influenced uranium fluid migration and deposition.

Porosity and permeability. Permeability barriers created by basement rocks and Sylhet Trap comprising porphyritic basalt with dominant plagioclase and clinopyroxenes (Sen et al., 2019). In addition to this, siltstone and clay-rich horizons resulting from the variation of sandstone grain size helped provide a permeability barrier so that the interaction of the U-rich solution can take place with the reductants. Fresh pulses of U-bearing fluids were brought to the basin due to the constant uplift of the Meghalaya Plateau. Further, the braided channel environment created favourable conditions that enhanced sandstone porosity, thereby causing transportation of U-rich fluid and its interaction with carbonaceous matter (Kaul & Varma, 1990).

Biological activity. Decomposition of plant material promoted uranium precipitation as coffinite and pitchblende, with biological processes indicated by the association of pyrite with uranium phases.

Cap rocks. Upper Mahadek sediments served as a cap rock, preserving uranium-rich Lower Mahadek sediments. Thick cap rocks were crucial for mineralisation, particularly in the eastern portion of the basin. The Upper Mahadek units consist of purple sandstones, glauconitic clays and shales with low permeability because of their texture and cementation. These act as seals preventing the movement of uranium-bearing fluids in upward direction and ensuring their entrapment and subsequent precipitation within the Lower Mahadek units. In the eastern sector, with increasing thickness of the cap, combined with fluvial structures, a favourable system of trap and reductant is formed.

Two major modes of occurrence of secondary uranium are seen in the basin, i.e., a) in the oxidised or weathered zones of primary mineral deposits wherein the alteration or decomposition of these primary minerals causes the formation of secondary minerals. In this case, the complete oxidation of the primary minerals may make it difficult to identify any primary structure. These are generally seen as oxidised vein deposits, and b) the second mode type corresponds to the transportation of uranium from the source rocks located at a distance and its subsequent precipitation from the solutions. In such a case, it occurs as irregular, flat-lying sandstone deposits, shale, limestone and conglomerate deposits. In this case, the precipitation of minerals is usually observed in fractures or veins.

Several factors are considered when selecting an area for U investigation, such as the age of the formation, the geological settings, the provenance, migration and uranium concentration. The uranium mineralisation found in Meghalaya is restricted to the Upper Cretaceous Mahadek formations, i.e., Lower Mahadek sandstones. The basement granitic rocks (Archean to Proterozoic) and Neoproterozoic granites are important provenance strata for uranium here (Srivastava et al., 2015). The Mahadek formations unconformably overlie basement rocks, and are overlain by Paleogene sediments. The primary U source is the basement crystalline rocks, while the Neoproterozoic granitoid near the uranium mineralisation sites helped enrich uranium. Archean to Proterozoic gneisses and granites are the primary sources inherently enriched in uranium. Neoproterozoic granitoids, such as the South Khasi Batholith, intruded later and are exposed near mineralised zones. These have been subjected to weathering and leaching under suitable oxidising

conditions. Being tectonically active, the Meghalaya Plateau resulted in a conductive environment, which helped the mechanical breakdown of the basement rocks. This was assisted by the presence of fresh feldspars in the Mahadek Formation and the release of uranium from the uranium phases and intergranular phases (Hamilton et al., 2010; Bhattacharjee et al., 2017). The Meghalaya Plateau´s continuous uplift provided the basin with fresh uranium-bearing fluids (Bhattacharjee et al., 2017). During the Late Cretaceous, the palaeoclimate was warm and humid, which is indicated by the existence of resin and carbonaceous matter. Thus, the palaeoclimate helped the oxidation and migration of uranium from the source rocks. The entrapment of uranium is caused by the solutions that carry the intrinsic uranium from nearby source rocks. Thus, under oxidising conditions where U^{4+} is oxidised to U^{6+}, it is mobilised by groundwater, which flows through the porous and permeable palaeochannel (Bhattacharjee et al., 2017). The uranium is reduced by carbonaceous matter and pyrite, which are the two dominant reductants (Kaul &Varma, 1990; Raju, 2019).

According to the study conducted by Rao et al. (1995) at Domiasiat, the abundant organic matter present can be segregated into six primary types and one secondary type, having different organic structures. The primary structures of organic matter are occupied mainly by uraninite, marcasite, pyrite and sphalerite. Organic matter maturation has formed secondary organic matter, which shows a transgressive relationship with primary organic matter. Apart from uraninite, coffinite and organo-uranyl complexes are also noticed in association with organic matter. The migration of leachable U is mainly by oxidised groundwater to the depositional sites, where reduction of uraninite and organo-uranyl complexes takes place. The former mineral forms due to reduction caused by bacteriogenic H_2S, while the latter forms because of complexation with organic matter. Further, coffinite precipitates during the organic acid maturation stage of organic matter. During this stage, various changes are observed, such as silica solubilisation, organo-silica formation, secondary organic matter, association of uranium with clay, and finally, partial replacement of uraninite with coffinite (Rao et al., 1995).

Thus, after major criteria for finding primary and secondary minerals are fulfilled based on the literature, an attempt can be made to study the identification and formation history of secondary uranium minerals in the study areas, as these have not yet been studied extensively. Thus, localities in the East Khasi and Jaintia districts that show U deposits or occurrences have been selected, with a few promising ones (Fig. 5; Raju, 2019).

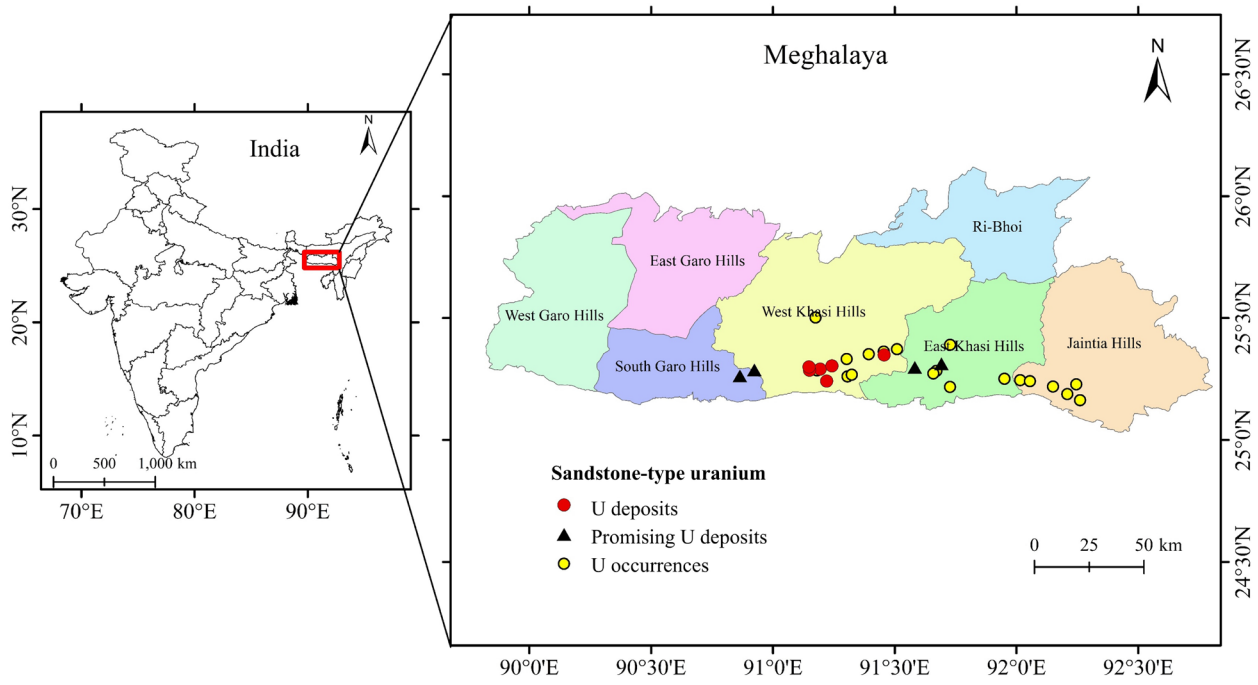

Fig. 5. Sandstone-type uranium deposits in Meghalaya, North-East India.

4. General methods for uranium exploration

Exploration for uranium deposits involves combining geophysical, geochemical and remote sensing techniques. These methods can be categorised into aerial surveys, field investigations and remote sensing approaches, each offering advantages in identifying potential uranium-rich zones.

4.1. Airborne surveys

Airborne surveys are cost-effective, enabling coverage of vast and often inaccessible terrains, while simultaneously acquiring multiple datasets. They offer high spatial accuracy and are widely used in reconnaissance studies. Gravity surveys detect variations in earth's gravitational field, indicative of dense rock formations potentially associated with uranium deposits (Zhang et al., 2022). Airborne gamma-ray spectrometry is particularly useful in detecting radioactive elements such as uranium (U), thorium (Th) and potassium (K) by measuring their characteristic gamma emissions (Nicolet & Erdi-Krausz, 2003).

4.2. On-site/ field surveys

Field surveys provide direct geological, geochemical and geophysical data crucial for understanding the mineralisation processes. These surveys include radiometric (Adepelumi & Falade, 2017), geophysical (Wu & Huang, 2021; Wu et al., 2022) and geochemical methods (Zhang et al., 2020). The field surveys include geological field work where various rock types belonging to a specific formation are noted, apart from the structural features. Field spectroscopy is very effective in acquiring spectral measurements (reflectance or emission) of rocks in the field, ranging between 0.35–14.00 μm. This is a suitable method for determining lithology and mineralisation in the field (Ramakrishnan & Bharti, 2015). Upscaling of the field spectroscopy is vital when its amalgamation with space/airborne hyperspectral images needs to be understood (Ramakrishnan & Bharti, 2015).

4.2.1. Radiometric method

Radiometric techniques such as γ-ray spectroscopy are a vital tool that help detect the anomalous zone and obtain assay values of U, Th and K. They are advantageous compared to the laboratory-based measurements, because they are capable of detecting radioactive elements immediately, and a vast area can be covered with handheld instruments. Thus, γ-ray survey facilitates geological formation mapping in terrain (Cassidy, 1981).

4.2.2. Geophysical method

Seismic surveys, mainly 3D seismic imaging, are instrumental in delineating uranium-bearing strata. Compared to 2D surveys, 3D seismic data provide high-resolution subsurface imaging, improving structural interpretations. For instance, a study by Wu & Huang (2021) in the Qiharigetu deposit (Erenhot Basin, China) demonstrated that 3D seismic methods effectively mapped lithology, fault structures and sandstone-hosted uranium mineralisation.

4.2.3. Geochemical method

Geochemical surveys analyse rock, soil and water samples to trace uranium and its environmental mobility. Uranium, soluble in oxidising groundwater, often forms geochemical halos near ore bodies (Langmuir & Chatham, 1980). Techniques such as inductively coupled plasma mass spectrometry (ICP-MS), gamma-ray spectrometry and alpha spectrometry facilitate the detection of uranium in various mediums (Leybourne et al., 2007; Bharti et al., 2015). In the Erlian Basin (China), geochemical analysis of fine-grained soil samples at 2-km-intervals revealed uranium mobility and potential mineralisation zones (Zhang et al., 2020). This underscores the importance of soil analysis in detecting concealed uranium deposits.

4.3. Remote sensing method

Remote sensing provides an indirect, yet consequential tool for uranium exploration by detecting alteration minerals and structural lineaments associated with uranium mineralisation. Multispectral (e.g., ASTER, Landsat) and hyperspectral (e.g., Hyperion, AVIRIS, HyMap, PRISMA) datasets facilitate mineral mapping based on spectral absorption features.

Hyperspectral imagery can detect key pathfinder minerals such as hematite, limonite, and chlorite, which indicate uranium-related hydrothermal alterations (dos Reis et al., 2017). Structural analysis through remote sensing aids in mapping faults and fractures that may act as fluid pathways for uranium transport and deposition (Aita & Omar, 2021). Digital Elevation Models (DEMs) also assist in reconstructing palaeochannels, which are crucial for locating roll front-type uranium deposits (Hou et al., 2017).

4.4. Positive effects and limitation of aerial gamma-ray spectrometry

Aerial gamma-ray spectrometry is a method in which a gamma-ray spectrometer is installed in a flying vehicle, enabling the measurement of energy spectra of radioactive elements (Jiang et al., 2023). This method has various benefits and positive effects that aid in the identification of potential uranium deposits of sandstone type. This cost-effective method offers speed and efficiency apart from a wide coverage, contributing to mineral exploration. It is not restricted by the terrain and acts advantageously, especially in regions such as the Mahadek Basin of India, which is characterised by inaccessible areas, thick forest, poor logistics and heavy precipitation. Further, this method is quick and measures the anomalous zones directly, which facilitates identification of uranium ore bodies. A case study conducted by Jiang et al. (2023) in the Gexi area of Inner Mongolia shows that the information produced by airborne gamma spectrometry served as a reliable indicator of ore bodies in the region.

Aerial gamma-ray spectrometry is an important tool for reconnaissance studies, but its effectiveness is limited in locating sandstone-type uranium deposits. These blinded or hidden deposits typically occur at depths beneath overburden or caprock. They may also be found lying under a highly weathered regolith, resulting in reduced surface radiometric anomalies. Another significant limitation is that the anomalies generated through gamma-ray spectrometry are lithologically controlled, as the rocks, such as granites with high inherent uranium content, can produce elevated radiation. Such false anomalies can be associated with resistant minerals, such as zircon or monazite, present in the rock and not leachable.The gamma-ray method is a surface mapping method, and it is seen that most of the gamma rays that emanate from the earth's surface are mainly from the top 30 cm (Nicolet & Erdi-Krausz, 2003). Thus, it cannot be used as a stand-alone method to identify sandstone-type deposits. The constraints can be overcome by using an integrated, multidisciplinary approach (Hegab, 2024).

4.5. Integrated approaches and advancements

Most uranium exploration programmes integrate multiple techniques for enhanced targeting accuracy. A study in the Kelâat M'Gouna region of Morocco combined airborne gamma-ray spectrometry with ASTER data to delineate hydrothermal alteration zones. These datasets were integrated into a GIS-based fuzzy logic model to produce mineral prospectivity maps (Mamouchet al., 2022).

Further, field-based reflectance spectroscopy is emerging as a precise method for uranium mineral identification. For instance, Hebert et al. (2019) demonstrated the quantification of coffinite using a Vis-NIR spectrometer, identifying diagnostic absorption bands at 1135 nm, 1418 nm, 1511 nm, 1678 nm and 2130 nm. Such spectroscopic techniques enable rapid field-based mineral identification, which is crucial for guiding further exploration.

Therefore, an attempt should be made to study the sandstone-type uranium deposits using advanced remote sensing methods (use of multispectral and hyperspectral images) in conjunction with

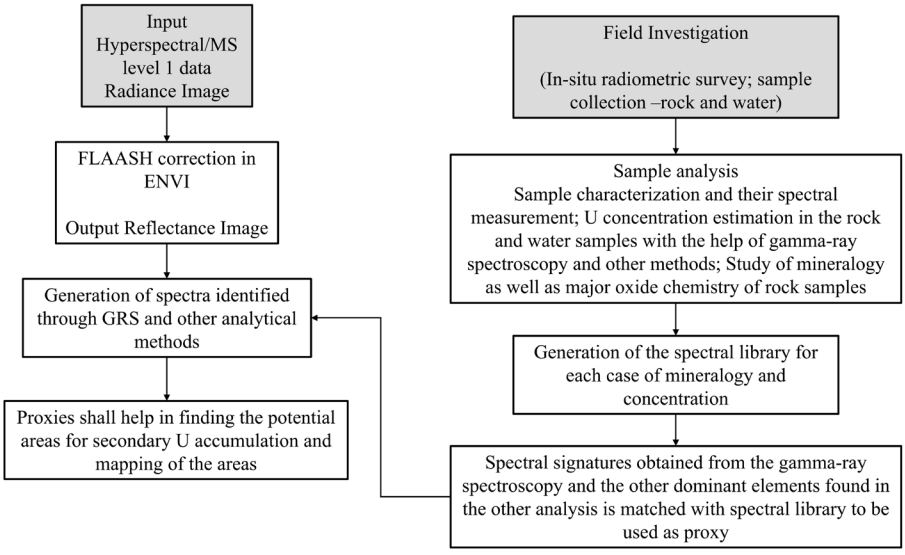

Fig. 6. General methodology that can be used for the study of sandstone-type uranium.

conventional techniques to not only understand the areas depicting the presence of primary uranium but also focus on the potentiality of any secondary uranium available in the area concerned. The following chart shows a general method that can be used to identify any secondary uranium present using remote sensing techniques and its validation by fieldwork (Fig. 6).

5. Conclusions

The present study provides a comprehensive review of the existing literature on sandstone-type uranium deposits, emphasising their geological settings and classification for the establishment of criteria for uranium potentiality. Identifying such deposits requires understanding geological formations, *in-situ* structural observations, lithology, stratigraphy, palaeoclimate, source and host rocks, transport mechanisms, depositional conditions and reductants. Uranium exhibits high geochemical mobility due to its polyvalence (+4, +6), large ionic radius and solubility variations, leading to primary mineralisation as uraninite and coffinite. These minerals form when uranium-rich rocks are brought to the surface and are exposed to weathering, where they become unstable and are leached by meteoric water or groundwater. The groundwater transports the uranyl solution to the deposition sites, where the change in redox state is due to enriched reductants. Subsequent environmental changes result in the formation of secondary uranium minerals such as uranocircite, autunite and uranophane due to multiple causes such as oxidation, hydrothermal alteration or direct precipitation.

In North-East India, the region's tectonic activity creates favourable conditions for secondary uranium formation, although processes governing its genesis remain poorly understood. Exploring uranium-bearing regions necessitates identifying expected uranium types and associated geological controls, with Hyperspectral Remote Sensing emerging as a valuable tool. Integrating Hyperspectral Remote Sensing with field-based investigations, including radiometric surveys and geochemical analyses, facilitates mineralogical mapping and upscaling of ground spectroscopic data to satellite scales. The numerous studies conducted in the Mahadek Basin of North-East India have synthesised the geological framework and mineralogical processes. The identification of primary and secondary uranium minerals has highlighted the complexities of the various factors involved such as provenance, redox state and hydrological conditions. Reductants, such as pyrite and carbonaceous matter, and permeability barriers and complex tectonics of the Meghalaya Plateau have played a significant role in the mobilisation, transportation and, finally, mineral precipitation. In North-East India, by establishing various structural, geological and geochemical parameters that help in the mineralisation process, the use of integrated exploration approaches should be considered. The detection and mapping of anomalous zones can be done by combining field-based data with optical or hyperspectral remote sensing, geochemical and radiometric surveys. A detailed understanding of the structures and mineralogy can provide a baseline for applying remote sensing techniques for the detection of unexplored regions with high uranium content under similar geological conditions. Understanding both primary and secondary uranium mineralisation mechanisms will enhance the application of advanced remote sensing techniques, enabling similar investigations in North-East India in attempts to locate new uranium-bearing areas based on geological and spectral characteristics.

References

Abzalov M.Z. & Paulson O., 2012. Sandstone hosted uranium deposits of the Great Divide Basin, Wyoming, USA. *Applied Earth Science* 121, 76–83.

Adepelumi A.A. & Falade A.H., 2017. Combined high-resolution aeromagnetic and radiometric mapping of uranium mineralization and tectonic settings in Northeastern Nigeria. *Acta Geophysica* 65, 1043–1068. https://doi.org/10.1007/s11600-017-0080-3.

Aita S.K. & Omar A.E., 2021. Exploration of uranium and mineral deposits using remote sensing data and GIS applications, Serbal area, Southwestern Sinai, Egypt. *Arabian Journal of Geosciences* 14, 1–17. https://doi.org/10.1007/s12517-021-08568-0.

Akhtar S., Yang X. & Pirajno F., 2017. Sandstone type uranium deposits in the Ordos Basin, Northwest China: A case study and an overview. *Journal of Asian Earth Sciences* 146, 367–382. https://doi.org/10.1016/j.jseaes.2017.05.028.

Alexandre P., Kyser K., Layton-Matthews D., Beyer S.R., Hiatt E.E. & Lafontaine J., 2015. Formation of the enigmatic Matoush uranium deposit in the Paleoprotozoic Otish Basin, Quebec, Canada. *Mineralium Deposita* 50, 825–845. https://doi.org/10.1007/s00126-014-0569-5.

Bankole O.M., El Albani A., Meunier A., Rouxel O.J., Gauthier-Lafaye F. & Bekker A., 2016. Origin of red beds in the Paleoproterozoic Franceville Basin, Gabon, and implications for sandstone-hosted uranium mineralization. *American Journal of Science* 316, 839–872. https://doi.org/10.2475/09.2016.02.

Bharti R. & Ramakrishnan D., 2014. *Uraniferous calcrete mapping using hyperspectral remote sensing*. IEEE Geosci-

ence and Remote Sensing Symposium, pp. 2902–2905. https://doi.org/10.1109/IGARSS.2014.6947083.

Bharti R., Kalimuthu R. & Ramakrishnan D., 2015. Spectral pathways for exploration of secondary uranium: An investigation in the desertic tracts of Rajasthan and Gujarat, India. *Advances in the Space Research* 56, 1613–1626. https://doi.org/10.1016/j.asr.2015.07.015.

Bhattacharjee P., Rengarajan M., Srivastava S.K., Hamilton S. & Mohanty R., 2017. Palaeochannel-controlled depositional features of the cretaceous lower Mahadek uranium Mineralisation in Umthongkut area, West Khasi Hills, Meghalaya. *Journal of the Geological Society of India* 90, 175–182. https://doi.org/10.1007/s12594-017-0696-6.

Billon S. & Patrier P., 2019. Diagenetic and hydrothermal history of the host rock of the Imouraren uranium deposit (Tchirezrine 2 Formation-Tim Mersoï Basin, Niger). *Journal of African Earth Sciences* 160, 103637. https://doi.org/10.1016/j.jafrearsci.2019.103637.

Bonnetti C., Cuney M., Michels R., Truche L., Malartre F., Liu X. & Yang J., 2015. The multiple roles of sulfate-reducing bacteria and Fe-Ti oxides in the genesis of the Bayinwula roll front-type uranium deposit, Erlian Basin, NE China. *Economic Geology* 110, 1059–1081. https://doi.org/10.2113/econgeo.110.4.1059.

Boyle R.W., 1982. *Geochemical prospecting for thorium and uranium deposits*. Elsevier, New York, 508 pp.

Cassidy J., 1981. Techniques of field gamma-ray spectrometry. *Mineralogical Magazine* 44, 391–398. https://doi.org/10.1180/minmag.1981.044.336.04.

Cazoulat M., 1985. *Geologic environment of the uranium deposits in the Carboniferous and Jurassic sandstones of the western margin of the Air Mountains in the Republic of Niger.* Report no. IAEA-TECDOC – 328, IAEA, Vienna, 408 p.

Covington J.H. & Kennelly P., 2018. Paleotopographic influences of the Cretaceous/Tertiary angular unconformity on uranium mineralization in the Shirley Basin, Wyoming. *Journal of Maps* 14, 589–596.

Cuney M., 2010. Evolution of uranium fractionation processes through time: driving the secular variation of uranium deposit types. *Economic Geology* 105, 553–569. https://doi.org/10.2113/gsecongeo.105.3.553.

Cuney M. & Kyser T.K., 2009. Recent and not-so-recent developments in uranium deposits and implications for exploration. Quebec. *Mineralogical Association of Canada* 39, 79–95.

Cuney M., Mercadier J. & Bonnetti C., 2022. Classification of sandstone-related uranium deposits. *Journal of Earth Sciences* 33, 236–256. https://doi.org/10.1007/s12583-021-1532-x.

Dahlkamp F.J., 1993. *Uranium Ore Deposits*. Springer, Berlin, 460 pp.

Dahlkamp F.J., 2009. *Uranium deposits of the world: Asia*. Springer, Berlin, 494 pp.

Dai S., Yang J., Ward C.R., Hower J.C., Liu H., Garrison T.M. French, D. & O'Keefe J.M., 2015. Geochemical and mineralogical evidence for a coal-hosted uranium deposit in the Yili Basin, Xinjiang, Northwestern China. *Ore Geology Reviews* 70, 1–30. https://doi.org/10.1016/j.oregeorev.2015.03.010.

Devillers C. & Menes J., 1977. *Dating of Akouta mineralization.* Supplement Report DRA/SAECNI/77, DR62/123/CD/DT1977. 7–15 pp.

Dos Reis Salles R., de Souza Filho C.R., Cudahy T., Vicente L.E. & Monteiro L.V.S., 2017. Hyperspectral remote sensing applied to uranium exploration: A case study at the Mary Kathleen metamorphic-hydrothermal U-REE deposit, NW, Queensland, Australia. *Journal of Geochemical Exploration* 179, 36–50. https://doi.org/10.1016/j.gexplo.2016.07.002.

Evans A.M., 2009. *Ore geology and industrial minerals: An introduction*. Blackwell, New Jersey, 389 pp.

Finch W.I., 1996. *Uranium provinces of North America: Their definition, distribution, and models*. US Government Printing Office no. 2141.

Finch W.I. & Davis J.F., 1985. *Sandstone-type uranium deposits.* Report No. TECDOC—328, IAEA, Vienna, 408 p.

Forbes P., 1988. *Rôles des structures sédimentaires et tectoniques, du volcanisme alcalin régional et des fluides dia génétiques-hydrothermaux pour la formation des minéralisations à U-Zr-Zn-V-MO d'Akouta (Niger).* PhD dissertation, University of Burgundy, Dijon, France.

Gauthier-Lafaye F., 2006. Time constraint for the occurrence of uranium deposits and natural nuclear fission reactors in the Paleoproterozoic Franceville Basin (Gabon). *Evolution of Early Earth's Atmosphere, Hydrosphere, and Biosphere: Constraints from Ore Deposits* 198, 157. https://doi.org/10.1130/2006.1198(09).

Gauthier-Lafaye F. & Weber F., 1989. The Francevillian (lower Proterozoic) uranium ore deposits of Gabon. *Economic Geology* 84, 2267–2285. https://doi.org/10.2113/gsecongeo.84.8.2267.

Gerbeaud O., 2006. *Evolution Structurale du Bassin de Tim Mersoï le Rôle des Déformations de la Couverture Sédimentaire sur la Mise en Place des Gisements Uranifère du Secteur d Arlit (Niger)*. PhD dissertation, Paris-Sud University, Orsay.

Hall S.M., Van Gosen B.S. & Zielinski R.A., 2023. Sandstone-hosted uranium deposits of the Colorado Plateau, USA. *Ore Geology Reviews* 155, 105353.

Hamilton S., Bhattacharjee P., Srivastava S.K., Rengarajan M., Majumdar A. & Mohanthy R., 2010. Geochemical approach in deciphering basinal development and uranium mineralization in parts of Mahadek basin, Meghalaya, India. *Geological Society India Memoir* 75, 165.

Hebert B., Baron F., Robin V., Lelievre K., Dacheux N., Szenknect S., Mesbah A., Pouradier A., Jikibayev R., Roy R. & Beaufort D., 2019. Quantification of coffinite (USiO4) in roll-front uranium deposits using visible to near infrared (Vis-NIR) portable field spectroscopy. *Journal of Geochemical Exploration* 199, 53–59. https://doi.org/10.1016/j.gexplo.2019.01.003.

Hegab M.A.E.R., 2024. A multi-disciplinary approach for uranium exploration using remote sensing and airborne gamma-ray spectrometry data in the Gebel Duwi area, Central Eastern Desert, Egypt. *Scientific Reports* 14, 19739.

Hou B., Keeling J. & Li Z., 2017. Paleovalley-related uranium deposits in Australia and China: A review of geo-

logical and exploration models and methods. *Ore Geology Reviews* 88, 201–234. https://doi.org/10.1016/j.oregeorev.2017.05.005.

International Atomic Energy Agency, 2009. *World distribution of uranium deposits (UDEPO) with uranium deposit classification.* Report TECDOC-1629, Vienna, 128 p.

International Atomic Energy Agency, 2020. *Descriptive uranium deposit and mineral system models*. Non-serial Publications, Vienna, 313 p.

International Atomic Energy Agency, 2021. *World distribution of uranium provinces.* Non-serial Publications, IAEA, Vienna.

Jaireth S., 2009. Uranium deposits of the Lake Frome region. Uranium ore-forming systems of the Lake Frome region, South Australia: regional spatial controls and exploration criteria. *Geoscience Australia Record* 40, pp. 57–79.

Jaireth S., McKay A. & Lambert I., 2008. Association of large sandstone uranium deposits with hydrocarbons. *AusGeo News*, Geoscience Australia 89, 1–6.

Jiang Z., Han X., Lin Z., Hu H., Lai Q., Gu Y., Wu Z. & Zhao X., 2023. Large-scale aerial gamma spectroscopy for exploring sandstone-type uranium deposits: A case study of Gexi Area, Inner Mongolia. *Applied Geophysics* 20, 1–12.

Kaul R. & Varma H.M., 1990. Geological evolution and genesis of the sandstone type Uranium deposit at Domiasiat, West Khasi Hills District, Meghalaya, India. *Exploration and Research for Atomic Minerals* 3, 1–16.

Langmuir D. & Chatham J.R., 1980. Groundwater prospecting for sandstone-type uranium deposits: a preliminary comparison of the merits of mineral-solution equilibria, and single-element tracer methods. *Journal of Geochemical Exploration* 13, 201–219. https://doi.org/10.1016/0375-6742(80)90007-2.

Lecomte A., Michels R., Cathelineau M., Morlot C., Brouand M. & Flotté N., 2020. Uranium deposits of Franceville basin (Gabon): Role of organic matter and oil cracking on uranium mineralization. *Ore Geology Reviews* 123, 103579. https://doi.org/10.1016/j.oregeorev.2020.103579.

Leybourne M.I., Cameron E.M. & Milkereit B., 2007. Groundwaters in geochemical exploration: methods, applications, and future directions. *Proceedings of Exploration* 7, 201–221.

Mamadou M.M., Cathelineau M., Deloule E., Reisberg L., Cardon O., Vallance J. & Brouand M., 2022. The Tim Mersoï Basin uranium deposits (Northern Niger): Geochronology and genetic model. *Ore Geology Reviews* 145, 104905. https://doi.org/10.1016/j.oregeorev.2022.104905.

Mamouch Y., Attou A., Miftah A., Ouchchen M., Dadi B., Achkouch L., Et-tayea Y., Allaoui A., Boualoul M., Randazzo G., Lanza S. & Muzirafuti A., 2022. Mapping of hydrothermal alteration zones in the Kelâat M'Gouna Region using airborne gamma-ray spectrometry and remote sensing data: Mining implications (Eastern Anti-Atlas, Morocco). *Applied Sciences* 12, 957. https://doi.org/10.3390/app12030957.

Nicolet J.P. & Erdi-Krausz G., 2003. *Guidelines for radioelement mapping using gamma ray spectrometry data.* International Atomic Energy Agency IAEA-TEC-DOC-1363, 179.

Penney R., 2012. Australian sandstone-hosted uranium deposits. *Applied Earth Science* 121, 65–75. https://doi.org/10.1179/1743275812Y.0000000018.

Petrov N.N., 1998. Epigenetic stratified-infiltration uranium deposits in Kazakstan. *Geologiya Kazakhstana* 6, 22–39.

Raju R.D., 2019. *Indian Uranium Deposits*. Cambridge Scholars Publishing, New Castle, 561 pp.

Ramakrishnan D. & Bharti R., 2015. Hyperspectral remote sensing and geological applications. *Current science* 108, 879–891.

Rao N.K., Sunilkumar T.S. & Narasimhan D., 1995. Uraniferous organic matter in the sandstone-type uranium ore from Domiasiat, Meghalaya, India. *Journal of the Geological Society of India* 45, 407–407.

Sen B., Pal T. & Theunuo K., 2019. Petrology and geochemistry of mafic dykes of Sylhet traps, Northeastern India, and their Kerguelen plume linkage. *Mineralogy and Petrology* 113, 783–801. https://doi.org/10.1007/s00710-019-00686-8.

Shi Z.Q., Yang X.K., Wang Y.Y., Du Y., Xiao K. & Duan X., 2016. Theory of uranium mineralization caused by supergene hydrothermal fluid in coal-bearing basins: Evidences from Jurassic sandstone in southern Yili Basin and North-eastern Ordos Basin. China. *Journal of Chengdu University of Technology* 43, 703–718.

Shi Z., Chen B., Wang Y., Hou M., Jin X., Song H. & Wang X., 2020. A linkage between uranium mineralization and high diagenetic temperature caused by coal self-ignition in the southern Yili Basin, North-western China. *Ore Geology Reviews* 121, 103443. https://doi.org/10.1016/j.oregeorev.2020.103443.

Skirrow R.G., Jaireth S., Huston D.L., Bastrakov E.N., Schofield A., Van der Wielen S.E. & Barnicoat A.C., 2009. *Uranium mineral systems: processes, exploration criteria and a new deposit framework.* Report: Geoscience Australia Record, 20, 44 p.

Spirakis C.S., 1996. The roles of organic matter in the formation of uranium deposits in sedimentary rocks. *Ore Geology Reviews* 11, 53–69. https://doi.org/10.1016/0169-1368(95)00015-1.

Srivastava S.K., Hamilton S., Nayak S., Pandey U.K., Mohanty R. & Umamaheswar K., 2015. Petrography, geochemistry and Rb-Sr geochronology of the basement granitoids from Umthongkut area, West Khasi Hills district, Meghalaya, India: Implications on petrogenesis and uranium mineralization. *Journal of the Geological Society of India* 86, 59–70. https://doi.org/10.1007/s12594-015-0281-9.

Turpina L., Clauer N., Forbes P. & Pagel M., 1991. U-Pb, Sm-Nd and K-Ar systematics of the Akouta uranium deposit, Niger. *Chemical Geology: Isotope Geoscience Section* 87, 217–230. https://doi.org/10.1016/0168-9622(91)90022-O.

Wu Q. & Huang Y., 2021. Indications of sandstone-type uranium mineralization from 3D seismic data: a case study of the Qiharigetu deposit, Erenhot Basin, Chi-

na. *Journal of Petroleum Exploration and Production* 11, 1069–1080.

Wu Q., Wang Y., Li Z., Qiao B., Yu X., Huang W. & Huang Y., 2022. 2D and 3D seismic survey for sandstone-type uranium deposit and its prediction patterns, Erlian Basin, China. *Minerals* 12, 559. https://doi.org/10.3390/min12050559.

Wülser P.A., Brugger J., Foden J. & Pfeifer H.R., 2011. The sandstone-hosted Beverley uranium deposit, Lake Frome Basin, South Australia: mineralogy, geochemistry, and a time-constrained model for its genesis. *Economic Geology* 106, 835–867. https://doi.org/10.2113/econgeo.106.5.835.

Zhang B., Wang X., Zhou J., Han Z., Liu W., Liu Q., Wang W., Li R., Zhang B. & Dou B., 2020. Regional geochemical survey of concealed sandstone-type uranium deposits using fine-grained soil and groundwater in the Erlian basin, North-east China. *Journal of Geochemical Exploration* 216, 106573. https://doi.org/10.1016/j.gexplo.2020.106573.

Zhang P., Yu C., Zeng X., Tan S. & Lu C., 2022. Ore-controlling structures of sandstone-hosted uranium deposit in the southwestern Ordos Basin: Revealed from seismic and gravity data. *Ore Geology Reviews* 140, 104590.

Manuscript submitted: 5 April 2025
Revision accepted: 27 July 2025